New Phytologist

Research

The root indeterminacy-to-determinacy developmental switch is operated through a folate-dependent pathway in *Arabidopsis thaliana*

Blanca Jazmín Reyes-Hernández[1], Avinash C. Srivastava[2], Yamel Ugartechea-Chirino[1], Svetlana Shishkova[1], Perla A. Ramos-Parra[3], Verónica Lira-Ruan[1], Rocío I. Díaz de la Garza[3], Gaofeng Dong[1], Jun-Cheol Moon[1], Elison B. Blancaflor[2] and Joseph G. Dubrovsky[1]

[1]Departamento de Biología Molecular de Plantas, Instituto de Biotecnología, Universidad Nacional Autónoma de México (UNAM), Apartado Postal 510-3, 62250 Cuernavaca, Mexico;

[2]Plant Biology Division, Samuel Roberts Noble Foundation, Ardmore, OK 73401, USA; [3]Escuela de Biotecnología y Alimentos, Centro de Biotecnología – FEMSA, Monterrey 64849, Mexico

Author for correspondence:
Joseph G. Dubrovsky
Tel: +52 7773291664
Email: jdubrov@ibt.unam.mx

Received: *19 November 2013*
Accepted: *2 February 2014*

New Phytologist (2014)
doi: 10.1111/nph.12757

Key words: determinate root growth, folate metabolism, lateral root formation, root apical meristem, stem cell niche, vitamin B9.

Summary

- Roots have both indeterminate and determinate developmental programs. The latter is preceded by the former. It is not well understood how the indeterminacy-to-determinacy switch (IDS) is regulated.
- We isolated a *moots koom2* (*mko2*; 'short root' in Mayan) *Arabidopsis thaliana* mutant with determinate primary root growth and analyzed the root apical meristem (RAM) behavior using various marker lines. Deep sequencing and genetic and pharmacological complementation permitted the identification of a point mutation in the *FOLYLPOLYGLUTAMATE SYNTHETASE1* (*FPGS1*) gene responsible for the *mko2* phenotype.
- Wild-type *FPGS1* is required to maintain the IDS in the 'off' state. When FPGS1 function is compromised, the IDS is turned on and the RAM becomes completely consumed. The polyglutamate-dependent pathway of the IDS involves activation of the quiescent center independently of auxin gradients and regulatory modules participating in RAM maintenance (WUSCHEL-RELATED HOMEOBOX5 (WOX5), PLETHORA, and SCARECROW (SCR)). The *mko2* mutation causes drastic changes in folate metabolism and also affects lateral root primordium morphogenesis but not initiation.
- We identified a metabolism-dependent pathway involved in the IDS in roots. We suggest that the root IDS represents a specific developmental pathway that regulates RAM behaviour and is a different level of regulation in addition to RAM maintenance.

Introduction

Operation of developmental mechanisms depends on housekeeping and general metabolism-related genes involved in maintenance of fundamental life functions. Not much is known, however, about how these genes interact with specific developmental pathways (Kooke & Keurentjes, 2012). During the last decade, genes have been identified whose functions are important for both general plant metabolism and some specific developmental programs (Chen & Xiong, 2005; Mo *et al.*, 2006; Mehrshahi *et al.*, 2010; Srivastava *et al.*, 2011a). One such gene, which encodes a folylpolyglutamate synthetase and is involved in vitamin B9-related metabolism, is essential for root apical meristem (RAM) function (Srivastava *et al.*, 2011a,b).

Vitamin B9 is a collective term for tetrahydrofolate (THF) and its derivatives, which are vital for basic metabolism because they are donors of the C1 atom during synthesis of essential cellular compounds such as amino acids, purines, thymidylate, pantothenate, and formylmethionyl–transfer RNAs (Fig. 1, Table 1). Monoglutamylated THFs are converted by folylpolyglutamate synthetases (FPGSs) to polyglutamylated THFs (Fig. 1b) which have greater stability, as they are less prone to oxidative cleavage (Ravanel *et al.*, 2001, 2011; Hanson & Gregory, 2011). In *Arabidopsis thaliana*, FPGS1/AtDFB is found in plastids, FPGS2/AtDFC in mitochondria, and FPGS3/AtDFD in the cytosol (Tables 1,2; Ravanel *et al.*, 2001; Mehrshahi *et al.*, 2010). Because mammals lack the folate biosynthetic machinery, they have to obtain this vitamin mainly from plant sources. Folate deficiency causes various developmental abnormalities during animal and plant development (Ishikawa *et al.*, 2003; Ifergan & Assaraf, 2008; Hanson & Gregory, 2011; Srivastava *et al.*, 2011a). For example, a mutation in *A. thaliana GLOBULAR ARREST1* which encodes a dihydrofolate (DHF) synthase (DHFS/AtDFA), involved in the synthesis of DHF, results in a developmental arrest at the globular-to-heart transition stage of embryo formation (Ishikawa *et al.*, 2003). Mitochondrial and cytosolic FPGS isoforms are required for embryogenesis and shoot/flower development, respectively (Mehrshahi *et al.*, 2010),

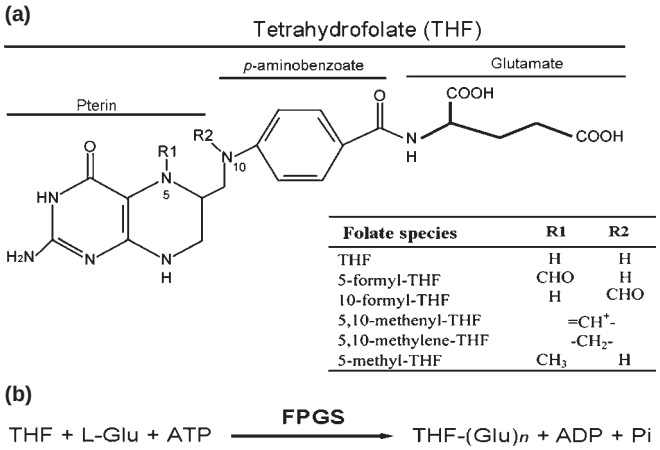

Fig. 1 Folate structure and reaction of polyglutamylation. (a) Tetrahydrofolate (THF) structure and related folate species. (b) Reaction of polyglutamylation catalyzed by FOLYLPOLYGLUTAMATE SYNTHETASE (FPGS).

whereas the plastidial isoform is essential for root growth and the maintenance of RAM activity (Srivastava *et al.*, 2011a,b).

In the root, two essential RAM components are important for the maintenance of growth. The first is a stem cell niche that includes quiescent center (QC) cells surrounded by the initial (stem) cells that give rise to different cell types (Van Den Berg *et al.*, 1997; Sabatini *et al.*, 2003; Aida *et al.*, 2004). The second is the cell proliferation domain where cells in the *A. thaliana* root pass through four to five cell division cycles before they start rapid elongation (Bennett & Scheres, 2010; Ivanov & Dubrovsky, 2013). RAM activity depends on the coordinated function of these compartments through complex gene regulatory networks. Root growth can be indeterminate or determinate. While the RAM is functional, indeterminate root growth is maintained. Under certain conditions, the RAM can be significantly diminished or consumed and the root stops growing (Perilli *et al.*, 2012; Xiong *et al.*, 2013). However, no determinacy program is turned on when a pool of meristematic cells is maintained to permit posterior growth recovery (Xiong *et al.*, 2013). However, when a determinate developmental program operates, the RAM eventually is completely consumed (exhausted), and root growth stops (Shishkova *et al.*, 2008).

The determinacy program leads to differentiation of all cells at the root apex, as observed in the primary roots of Cactaceae and in clustered or some unclustered lateral roots in many plant taxa, including agricultural crops (Varney & McCully, 1991; Watt & Evans, 1999; Shane & Lambers, 2005; Zobel, 2013). Determinate root growth can be constitutive (Shishkova *et al.*, 2008) or induced under conditions of low phosphate (Watt & Evans, 1999; Sánchez-Calderón *et al.*, 2005; Shane & Lambers, 2005; Cruz-Ramírez *et al.*, 2006; Svistoonoff *et al.*, 2007; Shishkova *et al.*, 2008). Both types have an adaptive significance, and commonly before RAM exhaustion, an indeterminate growth phase is present. The mechanism that regulates the indeterminacy-to-determinacy switch (IDS) is not well understood. It has been shown that, during induced root determinacy, low phosphate sensing turns on the IDS, which is dependent on pH and iron (Fe) availability and mediated by the multicopper oxidases LOW PHOSPHATE ROOT1 (LPR1) and LPR2 (Svistoonoff *et al.*, 2007), and associated with activity of phosphate-recycling cellular components (Cruz-Ramírez *et al.*, 2006). In Cactaceae,

Table 1 *Arabidopsis thaliana FOLYLPOLYGLUTAMATE SYNTHETASE* (*FPGS*) genes: their names, compartmentalization, and related mutants

FPGS-encoding genes	Enzyme localization	Reported mutants
FPGS1/AtDFB/MKO2	Plastid	*fpgs1*[1], *drh2/atdfb-1*[2], *atdfb-2*[2], *atdfb-3*[2], *mko2*[3]
FPGS2/AtDFC	Mitochondrion	*fpgs2*[1]/*atdfc*[2]
FPGS3/AtDFD	Cytosol	*fpgs3*[1], *atdfd*[2]

[1]Mehrshahi *et al.* (2010).
[2]Srivastava *et al.* (2011a).
[3]This study. Where the same mutant has been reported with two different names, they are separated by "/".

Table 2 Folate species that donate or accept C1 and the respective products synthesized in different compartments

	Products synthesized in		
Folate species	Plastid	Mitochondrion	Cytosol
Tetrahydrofolate (THF)	Glycine	Glycine	Glycine
10-formyl-THF	Formyl-methionyl-tRNA Purines Formate	Formyl-methionyl-tRNA Formate	Formate
5,10-methylene-THF	Thymidylate Serine	Thymidylate Pantothenate Serine	Thymidylate Serine
5-methyl-THF	Methionine	np	Methionine

np, no product synthesized. The data shown are based on Mehrshahi *et al.* (2010); Hanson & Gregory (2011); Ravanel *et al.* (2011); and Srivastava *et al.* (2011a,b).

RAM exhaustion is related to the absence or only transitory establishment of the QC post-germination (Rodríguez-Rodríguez *et al.*, 2003). It appears that the same factors that maintain the stem cell niche can be involved in the maintenance of indeterminacy. For example, the transcription factors SHORT-ROOT (SHR), SCARECROW (SCR), and PLETHORA (PLT) are essential for QC identity and maintenance. Accordingly, single *shr* and *scr* mutants and double *plt1 plt2* mutants show a determinate root meristem phenotype (Benfey *et al.*, 1993; Sabatini *et al.*, 2003; Aida *et al.*, 2004). *PLT* gene function is inter-related to auxin gradients in the root tip (Aida *et al.*, 2004). Consequently, this plant hormone is essential for indeterminacy maintenance. Double loss-of-function mutants in the *TRYPTOPHAN AMINOTRANSFERASE OF ARABIDOPSIS1* (*TAA1*) and *TRYPTOPHAN AMINOTRANSFERASE RELATED2* (*TAR2*) genes involved in auxin synthesis show complete RAM exhaustion (Stepanova *et al.*, 2008). Also, the cell cycle machinery, specifically CDC27B/HOBBIT and a cell cycle switch protein CCS52A2, which are functional components of anaphase promoting complex/cyclosome (APC/C), is involved. (Willemsen *et al.*, 1998; Pérez-Pérez *et al.*, 2008; Vanstraelen *et al.*, 2009). Until now, however, there have only been a few reports on the dependence of the IDS on a particular metabolic pathway (Cheng *et al.*, 1995; Vernoux *et al.*, 2000).

Here we report that a folate polyglutamate-dependent pathway is involved in the control of the transition from root indeterminacy to determinacy in *A. thaliana*. We have isolated a *moots koom2* (*mko2*) loss-of-function mutant, which is not affected in QC establishment post-germination. We found that the *mko2* mutant is a new mutant allele of *AtDFB* encoding the plastidial FPGS isoform (FOLYLPOLYGLUTAMATE SYNTHETASE1 (FPGS1)). We report novel mechanistic insights into how folate metabolism regulates the IDS. The primary root meristem of *mko2* is consumed within a short time. Our analysis indicates that the folate polyglutamate-dependent pathway is not related to SHR/SCR- and PLT-dependent regulatory pathways of RAM indeterminacy and that it is also involved in lateral root (LR) primordium morphogenesis.

Materials and Methods

Plant material and growth conditions

The *mko2* mutant was isolated from ethyl methanesulfonate (EMS)-mutagenized seeds of *Arabidopsis thaliana* (L.) Heynh., Landsberg erecta (Ler) accession (EMS-mutagenized seeds were kindly donated by J. Bowman, University of California, Davis, CA, USA). A total of 17 457 M2 plants were screened for abnormal root phenotypes in the same screen where *mko1* was isolated (Hernández-Barrera *et al.*, 2011). The *mko2* mutant was backcrossed three times and F3 and posterior progenies were used for phenotypic analysis and crosses with marker lines. The mutants *atdfb-1*, *atdfb-2*, *atdfb-3*, *atdfc* and *atdfd* (Mehrshahi *et al.*, 2010; Srivastava *et al.*, 2011a) and the transgenic lines *pWOX5::GFP* (Sarkar *et al.*, 2007), *pSCR::H2B::YFP* (Heidstra *et al.*, 2004), *pPLT1::CFP* (Galinha *et al.*, 2007), *pDR5rev::GFP* (Friml *et al.*, 2003), *AUX1*::*AUX1::YFP* (53), *pPIN3::PIN3::GFP* (Friml *et al.*, 2002b), *pPIN4::PIN4::GFP* (Friml *et al.*, 2002a), *pAGL42::GFP* (Nawy *et al.*, 2005), *QC25*, *QC184*, and *J2341* (Sabatini *et al.*, 2003) have previously been described. Seeds were sterilized and seedlings were grown as previously described (Hernández-Barrera *et al.*, 2011). 5-Formyl-5,6,7,8-tetrahydrofolic acid calcium salt (5-CHO-THF), methionine and methotrexate (Sigma-Aldrich) were used at final concentrations of 500 μM, 10 μM, and 25 nM, respectively. For auxin treatment, 3 d post-germination (dpg) seedlings were transferred to media supplemented with 1-naphthaleneacetic acid (NAA) at a range of concentrations.

In silico mapping of the *mko2* mutation

mko2 was crossed with Columbia-0 (Col) wild type (WT) to generate a mapping population of the F_2 progeny. A nuclear-enriched DNA sample was prepared from *c.* 700 seedlings with a mutant phenotype from the mapping population (Schneeberger *et al.*, 2009). The Illumina library was sequenced at the UNAM DNA Deep Sequencing Facility (UUSMD-UNAM) (Cuernavaca, Mexico) to 15-fold genome coverage. The SHORE-MAP computer program was used for analysis of polymorphisms associated with the mutation (Schneeberger *et al.*, 2009).

Root growth, microscopy, and other analyses

Primary root length was measured on scanned images of seedlings using IMAGEJ software (http://rsb.info.nih.gov/ij/). The number of cortical cells within the RAM cell proliferation domain was determined on cleared root preparations in accordance with previously described criteria (Ivanov & Dubrovsky, 2013). Roots were cleared as previously described (Dubrovsky *et al.*, 2009) and analyzed under a Zeiss Axiovert 200M microscope (Zeiss, Oberkochen, Germany) equipped with differential interference contrast (Nomarski) optics. The LR density and initiation index were estimated as previously described (Dubrovsky *et al.*, 2009). Starch granules were stained as previously described (Hernández-Barrera *et al.*, 2011). Photographs were taken using a Photometrics CoolSNAPcf Color Camera (Valley International Corporation, Austin, TX, USA). Confocal microscopy was performed with a Zeiss LSM 510 Meta microscope; the laser setting was as described by Hernández-Barrera *et al.* (2011). For examination of cellular organization, roots were counterstained with propidium iodide (10 or 15 $\mu g\ \mu l^{-1}$) or FM4-64 (8 μM). Folate analyses were performed as previously described (Srivastava *et al.*, 2011a). Gene co-expression analysis was performed using GENEVESTIGATOR (Zimmermann *et al.*, 2004). Statistical analyses were performed as indicated in the figure legends.

Image analysis

As a consequence of differences in optical properties between the WT and mutant samples, we modified the images post-capture to improve the display of the signal distribution. These image modifications were performed linearly using IMAGEJ so that no information was lost. The original images are available upon

request. The mean pixel density of fluorescent signal was measured with ImageJ on original images obtained with identical laser settings.

Transcript level analysis

Total RNA was isolated from 11-d-old seedlings using an RNeasy mini kit (Qiagen, Hilden, Germany), according to the manufacturer's instructions. For quantitative two-step RT-PCR, 1 μg of total RNA was reverse-transcribed to first-strand cDNA with the Qiagen cDNA synthesis kit and this cDNA was subsequently used as a template for quantitative PCR with gene-specific primers. The plant-specific eukaryotic translation initiation factor *EIF4A2* gene served as a control for transcript level normalization, and comparative expression levels ($2^{-\Delta C_t}$) were calculated according to Ramakers *et al.* (2003). The primers used were as follows: *EIF4A2* (sense 5′-GGCTGAATGAA GTTCTCGATGGACAG-3′ and anti-sense 5′-ACGAGAGCCTGGCACTGGAGAAG-3′); *AtFPGS1* (sense 5′-GGTACAGC AGCTGATTTGC-3′ and anti-sense 5′-TCTTTCACTCTGCACAAGGC-3′); *AtFPGS2* (sense 5′-GGG GCTTGACCATACACTGA-3′ and anti-sense 5′- CAATGTG GTGGACCTGCAG-3′); *AtFPGS3* (sense 5′-CAGACAAACGG TTTACCCGA-3′ and anti-sense 5′-GAAAACGAACTTGTTT ACTTTGGC-3′).

Plasmid construction

All constructs were made using Gateway™ technology (Invitrogen Life Technologies, Carlsbad, CA, USA). The entry clones were obtained using the pENTR-D-TOPO vector (Invitrogen Life Technologies) and expression vectors using the Gateway vectors (Curtis & Grossniklaus, 2003). For complementation studies, a 7-kb genomic *FPGS1* fragment was amplified using gene-specific primers (sense 5′-TGTTAAGGTC AAAACATAAA CTCCAT-3′ and anti-sense 5′-TTTTCTGATTAATCTCAG TACATCGC-3′). This fragment is comprised of a 2-kb upstream *FPGS1* promoter region and a 5-kb region downstream of the ATG start codon. It was cloned into the pMDC107 binary vector, transformed into *Agrobacterium tumefaciens* LBA4404 and finally transformed into *mko2* and *atdfb1* mutants using the floral-dip method (Clough & Bent, 1998). Transgenic plants were selected on growth media supplemented with 25 μg ml^{-1} hygromycin and later propagated on soil. Around 10 independent T2 transgenic lines were tested for fluorescence and complementation.

Results

FPGS1 is required for indeterminate root growth

Based on morphological abnormalities of root system formation, we isolated an EMS-induced mutant with a very short primary root exhibiting determinate growth, and fewer and shorter LRs compared with wild type (WT) (Fig. 2a–c). The recessive mutant showed Mendelian inheritance and was denominated *moots koom 2* (*mko2*), which means 'short root' in the Mayan language. The *mko1* mutant has previously been described (Hernández-Barrera *et al.*, 2011).

The primary root of the *mko2* plants grew very slowly. By 8 dpg, primary roots averaged 5 mm in length, whereas the primary root of the WT Ler seedlings at this age was 10-fold longer (Fig. 2b). Determinate growth of the *mko2* primary root was caused by complete meristem consumption involving cessation of proliferation and terminal differentiation of the root tip cells. This could be detected morphologically by the presence of root hairs at the very tip of the primary root formed by differentiated epidermal cells (Fig. 2c).

The primary root was often intertwined with lateral and adventitious roots. Frequently, LRs were formed almost at the very tip of the primary root, whose growth had terminated (Fig. 2c) and for this reason the primary root could only be unambiguously identified until 10–12 dpg. As expected, a decrease in the number of meristematic cells compared with WT (Fig. 2d) was detected during the course of RAM exhaustion. It was a relatively rapid and asynchronous process and by 9 dpg RAM exhaustion was found in 61% of the *mko2* seedlings (Fig. 2e), whereas no seedlings of the same age without RAM were detected in WT.

To identify the gene responsible for the mutant phenotype, a nuclear DNA-enriched sample prepared from plants with the mutant phenotype from the mapping population was subjected to deep sequencing. Using SHORE-map software, the 'interval' plot of the relative allele frequencies of Ler and Col revealed a narrow candidate region (Fig. 2f). One candidate gene within this region, At5g05980, which encodes the plastidial isoform of FOLYLPOLYGLUTAMATE SYNTHETASE (FPGS1/AtDFB) (Ravanel *et al.*, 2001; Mehrshahi *et al.*, 2010; Srivastava *et al.*, 2011a), had a C to T transition in the 14th exon leading to an R445Q change in the C-terminal domain (Fig. 2g). Interestingly, in the allelic mutant *atdfb-3* in the Col background (Srivastava *et al.*, 2011a), the incidence of seedlings with determinate root growth was much lower, although root growth dynamics and meristem length were similar between *mko2* and *atdfb-3* seedlings, in contrast to the *atdfc* (*fpgs2*) and *atdfd* (*fpgs3*) mutants in other FPGS isoforms (Fig. 2b,d). This suggested specific roles for FPGS1, and not FPGS2 and FPGS3, in root development. Also, fully elongated cells in *mko2* were about two-fold shorter than those in WT, similar to those of plants of the *atdfb-3* mutant (Srivastava *et al.*, 2011a). Interestingly, the meristem exhaustion phenotype was found in the primary root but not in lateral roots of the *mko2* mutant. The shoot growth of the *mko2* mutant was slower in young plants but later these differences were less pronounced (Supporting Information Fig. S1a–d). The mutant produced functional inflorescences and viable seeds.

Exogenous application of 5-CHO-THF to *mko2* seedlings re-established primary root growth and normal RAM organization (Fig. S1f,g), as it does for other allelic mutants (Srivastava *et al.*, 2011a). Furthermore, the WT *FPGS1* genomic region complemented root developmental defects of the *mko2* mutant (Fig. S1e). Overall, this analysis suggested that the plastidial isoform, *FPGS1/AtDFB*, was required for indeterminate root growth and normal root development.

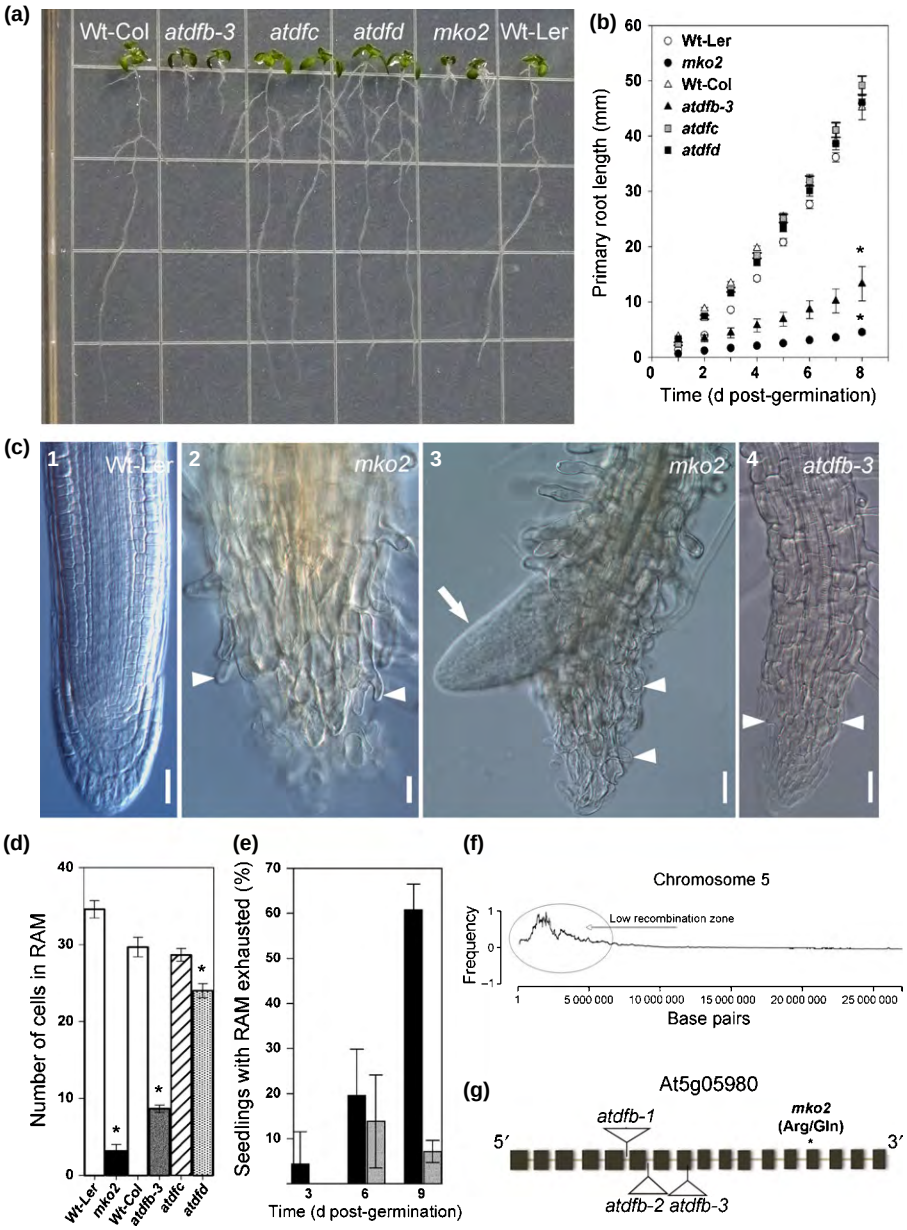

Fig. 2 Phenotype of the *Arabidopsis thaliana moots koom2* (*mko2*) mutant and other *folylpolyglutamate synthetase* (*fpgs*) mutants and *mko2* mapping. (a) Root system in mutants affected in *FPGS1* (*mko2* and *atdfb-3*), *FPGS2* (*atdfc*) and *FPGS3* (*atdfd*); *mko2* is in the wild-type Ler (Wt-Ler) and all other mutants are in the wild-type Col (Wt-Col) background; seedlings shown are 8 d post-germination (dpg). The length of a square side is 13.2 mm. (b) Dynamics of primary root growth (mean ± SE; $n = 20$–35). Statistically significant differences are indicated only for seedlings at 8 dpg; *, $P < 0.001$, Student's *t*-test. (c) The root tip phenotype in the Wt-Ler, *mko2*, and *atdfb-3* mutants at 6 (panels 1–2) and 11 (panels 3–4) dpg. Arrowheads, formation of root hairs at the very tip; arrow, emerging lateral root close to the tip of the primary root apex. Bars, 30 μm. (d) Root meristem length expressed as the number of cortical cells in a file within the cell proliferation domain of the root apical meristem (RAM) in seedlings at 6 dpg (mean ± SE; $n = 20$). Statistically significant differences were determined using Student's *t*-test: *, $P < 0.05$. (e) The dynamics of RAM exhaustion in *mko2* (black bars) and *atdfb-3* (gray bars); three biological replicates, 54–104 seedlings each (mean ± SE); the complete RAM exhaustion events of the primary root depicted in (c, panels 2–4) were scored. (f) Parental allele recombination frequency in a DNA sample of the *mko2* mapping population analyzed with SHORE-map after deep sequencing. (g) Schematic diagram of the coding sequence of *FPGS1*/*AtDFB* and position of *mko2* and the T-DNA insertion sites of known alleles.

The point mutation in *mko2* drastically affects folate metabolism

The mutation in *mko2* caused an R445Q change. The Arg in the corresponding position is highly conserved in plants and metazoans (Fig. S2) but not in some bacteria and fungi, and is located close to the FPGS catalytic domain. In humans, the equivalent Arg377 is important for the FPGS activity (Sanghani *et al.*, 1999). It was shown that the R377A mutation resulted in a 20-fold decrease in FPGS catalytic activity (Sanghani *et al.*, 1999). This analysis strongly suggests that the R445Q mutation in *FPGS1* should significantly affect protein function in the *mko2* mutant and subsequently changes the balance between mono- and polyglutamylated folates.

To test this hypothesis, we analyzed the folate profile separately for shoots and roots. Total folate contents remained similar; however, folate derivatives in *mko2* shoots and roots changed significantly in comparison with WT levels (Fig. 3a,b). In the *mko2* shoots, the monoglutamylated form of 5-CH3-THF decreased by 60% compared with WT (Fig. 3a). Polyglutamylated forms of THF (which includes 5,10-CH2-THF in our analysis) were only 15% of those in WT. Total folate contents remained similar as a result of a 1.6-fold increase in 5,10-CH=THF. In the *mko2* roots, the monoglutamylated form of 5-CH3-THF decreased by 40% compared with WT (Fig. 3b). THF contents increased greatly in the *mko2* mutant; the monoglutamylated THF was 680% of that in WT whereas monoglutamylated 5-CHO-THF increased to a much lesser extent. Surprisingly, a 6.9-fold increase was found in the polyglutamylated 5-CHO-THF form in the *mko2* roots. Although total folate content was similar in Ler (this study) and Col WT seedlings (Srivastava *et al.*, 2011a), we found that the extent of

polyglutamylated folates was less prevalent in the Ler background. In the Col WT roots, 78% of total folates were polyglutamylated (Srivastava *et al.*, 2011a), whereas in Ler WT only 38% were polyglutamylated (this study). Considering the polyglutamylated folates in *atdfb-1* and *mko2* versus the respective WTs, we estimated that, while *atdfb-1* roots contained 69% of that of the Col WT (Srivastava *et al.*, 2011a), the *mko2* roots had only 21% of that of the Ler WT. Overall, this analysis revealed that the FPGS1 defect in the *mko2* mutant significantly affected the balance between mono- and polyglutamylated folate species and that FPGS1 activity was compromised.

Previously, it was reported that the loss-of-function *atdfb-1*, *atdfb-2*, and *atdfb-3* mutants had no detectable *FPGS1* transcript (Srivastava *et al.*, 2011a). RT-qPCR analysis demonstrated that the *mko2* mutation did not abolish FPGS1 transcription but reduced the transcript level to *c.* 33% of that in WT (Fig. 3c). Importantly, the *mko2* mutation significantly affected the transcript level of the mitochondrial *AtDFC/FPGS2* and cytoplasmic *ATDFD/FPGS3* isoforms, diminishing it by *c.* 50% (Fig. 3c). These data suggested a feedback regulation of these genes by folates.

FPGS1/AtDFB function is required for indeterminate root growth through the maintenance of stem cell niche organization

To address how folate metabolism can be involved in RAM activity maintenance and the IDS, we analyzed developmental changes in the organization of the stem cell niche of the RAM. The *mko2* primary root had normal RAM organization in early post-germination seedlings (e.g. Fig. 4a,f, column 2), but gradual developmental changes led to RAM disorganization at later stages. Because meristem exhaustion was an asynchronous process (Fig. 2e) and it was difficult to identify the primary root in the *mko2* seedlings after 10–12 dpg, we focused on developmental changes taking place over a 9-dpg period. Using results for different individual roots, we proposed a scenario in which a sequence of events leads to RAM exhaustion; this sequence is depicted in

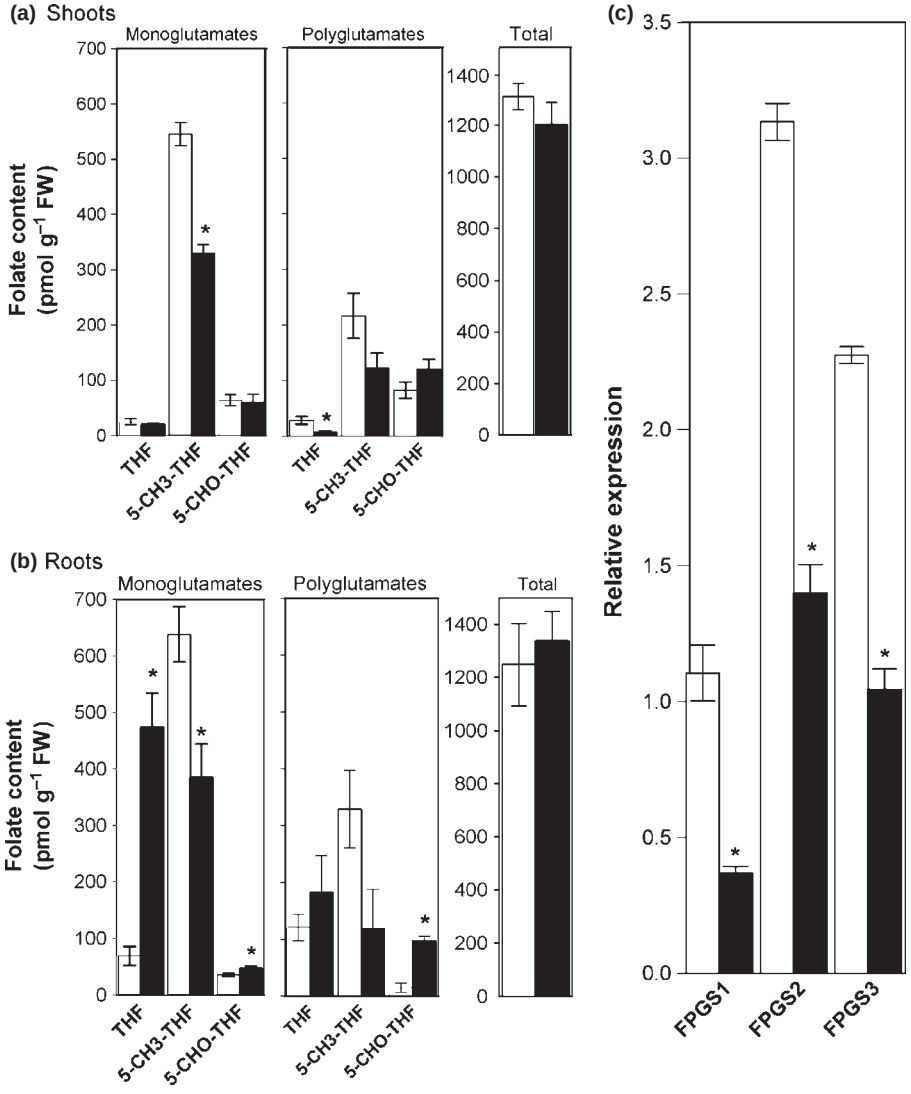

Fig. 3 Altered folate glutamylation profile and *FOLYLPOLYGLUTAMATE SYNTHETASE1* (*FPGS1*), *FPGS2* and *FPGS3* mRNA levels in the *Arabidopsis thaliana moots koom2* (*mko2*) mutant. (a, b) Folate glutamylation profile in shoots (a) and roots (b) of seedlings at 15 d post-germination (dpg). Data are mean ± SE from three biological replicates; each shoot sample included 50 seedlings and each root sample 150 seedlings. (c) RT-qPCR analysis of *FPGS1*, *FPGS2* and *FPGS3* expression in wild type (WT) and *mko2* seedlings at 11 dpg. Open bars, WT; closed bars, *mko2* mutants. Values are the mean ± SE of three biological and three technical replicates. Statistically significant differences were determined using Student's *t*-test: *, $P < 0.05$.

Fig. 4 (columns 2–4). When RAM exhaustion was over, it was practically impossible to analyze the roots with differentiated root tip cells under a confocal laser scanning microscope because of poor laser beam penetration into the tissues. For this reason, no data on roots with consumed RAM were obtained.

WUSCHEL-RELATED HOMEOBOX 5 (*WOX5*) is specifically expressed in the QC and is important for maintenance of distal stem (columella initial) cell activity (Sarkar *et al.*, 2007). In the *mko2* background, the domain of *WOX5* promoter activity was expanded (Fig. 4a, panels 1–4): GFP fluorescence was detected in 4.0 ± 1.9 and 2.4 ± 0.5 cells per confocal section in the *mko2* mutant and WT, respectively (mean $\pm$ SD; $n = 14–23$; Mann–Whitney rank sum test; $P < 0.001$). This implies that the FPGS1-dependent folate profile is important for maintaining the relative quiescence of the QC. Before RAM exhaustion, the *mko2* mutant showed the presence of starch granules in the columella initial cells (Fig. S3a), indicating their differentiation and loss of stem cell activity, similar to findings in *wox5-1* (Sarkar *et al.*, 2007) and *ccs52a2* (Vanstraelen *et al.*, 2009) mutants. This suggests that WOX5 function in the maintenance of distal stem cell activity was abolished in the *mko2* seedlings. In spite of differentiation, columella initial cells and their daughters maintained their identity, as demonstrated by J2341 enhancer trap GFP expression in the *mko2* background (Fig. S3b). Importantly, *pWOX5::GFP* expression was detected until the beginning of RAM exhaustion, suggesting that cells with QC identity were present while the RAM was maintained. This analysis showed that FPGS1-dependent maintenance of root indeterminacy can be *WOX5* mediated and that it can be related to loss of the proliferative quiescence of the QC.

The GRAS (*GIBBERELLIN-INSENSITIVE [GAI]*, *REPRESSOR of ga1-3 [RGA]*, *SCARECROW*) family transcription factor SHR moves out of the provascular tissues to the endodermis, the cortex-endodermis initial cells, and the QC, where it activates transcription of another member of the same family, *SCR*, which is essential for stem cell niche activity and maintenance of root indeterminacy (Nakajima *et al.*, 2001; Sabatini *et al.*, 2003). In the *mko2* background, no changes in *SCR* promoter activity were observed (Fig. 4b, panels 1–4), which is consistent with the phenotype observed in the *atdfb-1* allele (Fig. S4). When the QC cells divided periclinally, the *pSCR::H2B::YFP* marker was present in both cell layers in both allelic mutants. Similar to *WOX5*, *pSCR* activity was detected until RAM consumption.

Other important players in QC specification are the *PLT1* and *PLT2* genes from the APETALA2/Ethylene Responsive Factor (AP2/ERF) transcription factor family; they are required for stem cell activity and are redundantly involved in the preservation of root indeterminacy (Aida *et al.*, 2004; Galinha *et al.*, 2007). When *WOX5* is mutated it accelerates determinate development in both *scr-4* and *plt1 plt2* (double) mutants (Sarkar *et al.*, 2007), demonstrating that all three pathways apparently act synergistically to maintain indeterminate root growth. In the *mko2* mutant, *PLT1* promoter activity was similar to that in WT and was present until complete loss of the RAM (Fig. 4c, panels 1–4). Interestingly, the same behavior of the QC markers was found in the *atdfb-1* mutant. QC25 and QC184 (Sabatini *et al.*, 1999), *pAGL42::GFP* (Nawy *et al.*, 2005) and *pSCR::H2B-YFP* expression was found to be maintained until RAM disorganization (Fig. S4d). This analysis suggests that the folate pathway of root meristem indeterminacy control is independent of SCR-SHR- and PLT-dependent regulatory modules involved in stem cell niche maintenance. At advanced stages, before complete meristem exhaustion, all the markers analyzed in *mko2* were barely detected as a result of RAM disorganization (data not shown).

During the first 9 dpg, the QC in *mko2* showed periclinal divisions (e.g. Fig. 4a–e, column 3). While the QC cells are commonly transversely aligned in WT, the *mko2* mutant at 6–9 dpg exhibits a loss of alignment leading to the RAM disorganization that took place before meristem exhaustion. Analysis of *pWOX5::GFP* suggested that root determinacy in *mko2* is associated with proliferation activity of the QC cells. To test this hypothesis, we analyzed QC behavior in *mko2*. In WT, the QC cells divide rarely and in young seedlings the QC is commonly one cell layer thick (Bennett & Scheres, 2010). In *mko2* at 2–3 dpg, the QC thickness (height), expressed as number of cells, was the same as in WT and by 6 dpg it was close to two cells in height. This was 27% greater than in WT (Fig. 5a), suggesting that periclinal divisions in the QC were more frequent in the mutant. Remarkably, in spite of the absence of differences in the number of cells in seedlings at 2–3 dpg (Fig. 5b), the QC thickness increased in unit length and was 41% greater in *mko2* compared with WT, indicating unusual longitudinal growth of the QC cells. The same differences were found in plants at 6 dpg (Fig. 5a). These results showed that both activation of QC cell proliferation and their longitudinal expansion were abnormal in *mko2*. Lack of quiescence in the QC could inhibit stem cell functions, promote their differentiation and eventually lead to RAM exhaustion.

FPGS1/AtDFB is required for indeterminate root growth independently of auxin gradients

RAM organization and stem cell activity depend on auxin gradients established in the apex (Friml *et al.*, 2004; Blilou *et al.*, 2005) with a maximum in the QC (Sabatini *et al.*, 1999; Petersson *et al.*, 2009). A loss of the auxin maximum in the RAM leads to its consumption (Friml *et al.*, 2004). Monitoring of the auxin response with *DR5rev::GFP* showed that, while the QC cells divided periclinally in *mko2*, *DR5rev::GFP* fluorescence was found in the QC cell daughter cells and was maintained in the columella. Even in *mko2* seedlings at 9 dpg, when stem cell niche organization was significantly altered, the *DR5rev::GFP* expression pattern was conserved (Fig. 4d, panels 1–4). There was no difference in GFP signal intensity in *mko 2* versus WT (Fig. 4d, insets in panels 2 and 3). An essentially similar *DR5rev::GFP* expression pattern, although in fewer cells, was reported for the allelic *atdfb-1* mutant (Srivastava *et al.*, 2011a) in which determinate growth was only found in a small fraction of seedlings (Fig. 2e). These results suggested that the auxin gradients established in the root tip were not abolished. To test this hypothesis, we analyzed the expression pattern of *pAUX1::AUX1::YFP* (Swarup *et al.*, 2001), *pPIN3::PIN3::GPF* (Friml *et al.*, 2002b), and *pPIN4::PIN4::GPF* (Friml *et al.*, 2002a) markers and found that,

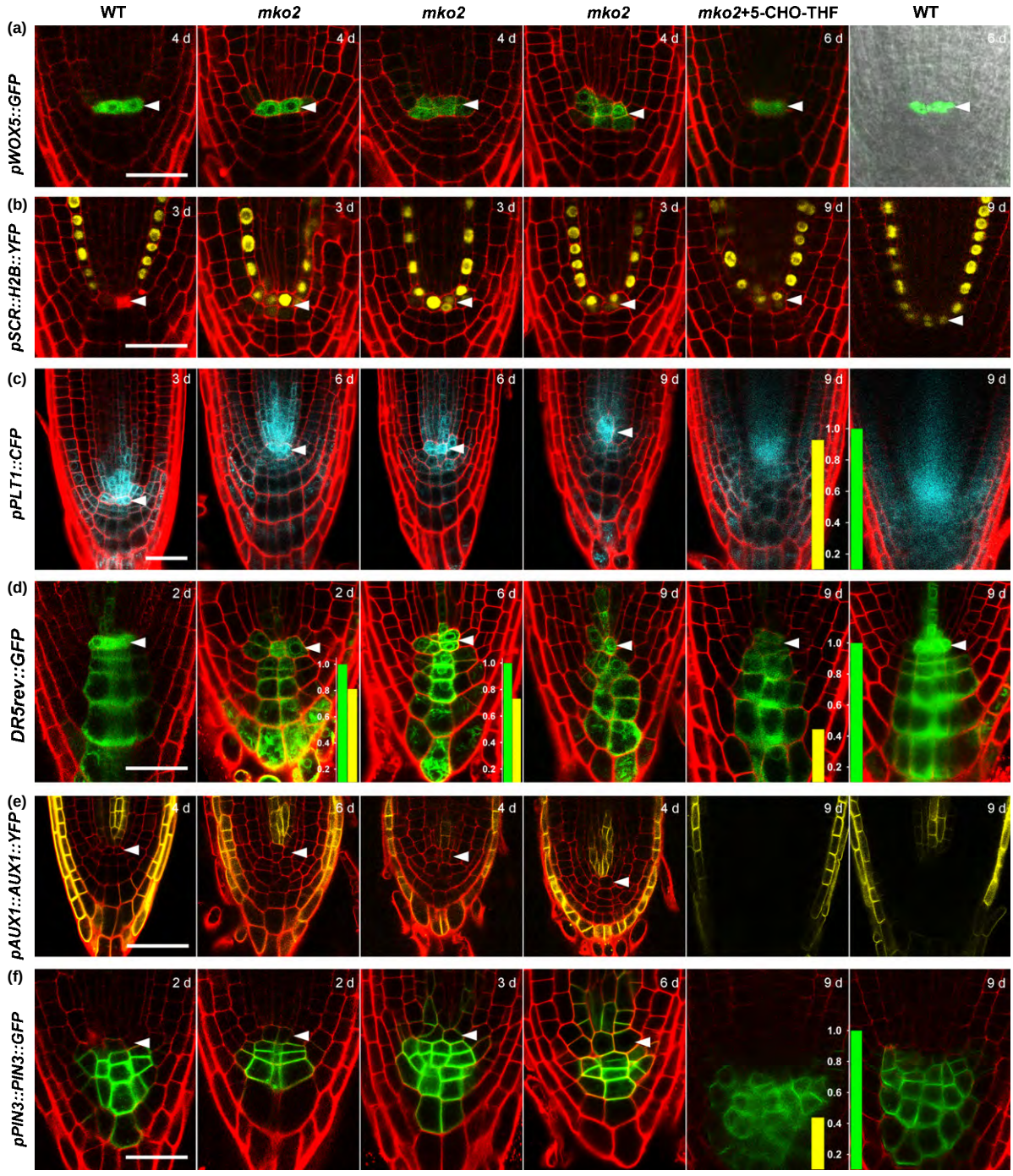

Fig. 4 Disorganization of the *Arabidopsis thaliana moots koom2* (*mko2*) root apical meristem, and expression of various markers with and without monoglutamylated tetrahydrofolate treatment. Expression of (a) *pWOX5::GFP*, (b) *pSCR::H2B::YFP*, (c) *pPLT1::CFP*, (d) *DR5rev::GFP*, (e) *pAUX1::AUX1::YFP* and (f) *pPIN3::PIN3::GFP* markers was analyzed. The first column shows the wild type (WT) roots. Columns 2–4 show developmental changes over a 9 d post-germination (dpg) period leading to root apical meristem (RAM) exhaustion; seedling age is indicated (d corresponds to days post-germination). As RAM exhaustion was asynchronous, at the same age a more or less advanced RAM consumption stages can be found. The fifth column shows the seedlings at 9 dpg (except for *pWOX5::GFP*, 6 dpg) germinated and grown in the medium supplemented with 500 μM 5-formyl-tetrahydropholate (5-CHO-THF). The sixth column shows untreated control seedling roots of the same age. Arrowheads indicate the quiescent center. For each marker line, age and condition, $n = 10–13$, except for the data shown in the last two columns ($n = 5$). All insets shown in columns 5 and 6 show quantification of fluorescent signal in respective marker lines ($n = 5$); in all cases no significant difference was found ($P > 0.05$; Student's *t*-test). Insets in (d), panels 2 and 3 show quantification of fluorescence signal in grouped samples of seedlings at 2–3 and 6 dpg, respectively; $n = 11–13$; no significant difference was found ($P > 0.05$; Student's *t*-test). Green bar, WT; yellow bar, *mko2*. Bars, 30 μm.

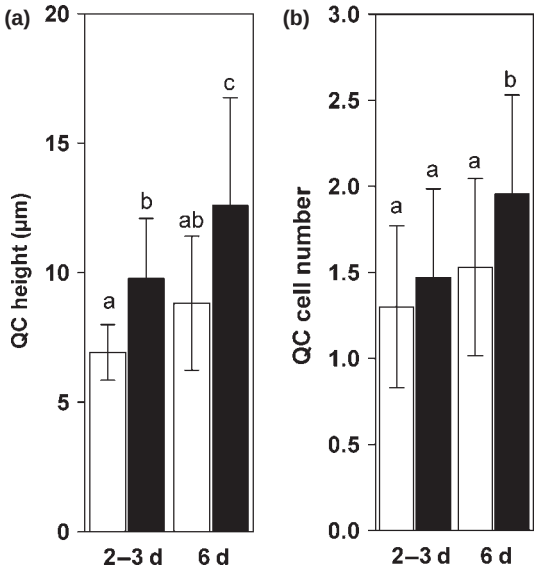

Fig. 5 The quiescent center (QC) size is altered in the *Arabidopsis thaliana moots koom2* (*mko2*) mutant compared with wild type (WT). (a) The QC thickness (height) expressed in micrometers. (b) The QC thickness expressed as the number of cells along the longitudinal axis; d corresponds to days post-germination; open and closed bars indicate WT and *mko2* mutants, respectively. Mean ± SD; $n = 17–22$; different letters indicate statistically significant differences following ANOVA multiple comparison Tukey test at $P < 0.05$.

while the RAM was preserved, the expression pattern for the AUX1 influx carrier was similar to that in WT (Fig. 4e, panels 1–4). PIN-FORMED 3 (PIN3) and PIN4 efflux carriers are important for stem cell niche patterning and correct RAM organization (Friml *et al.*, 2002a; Blilou *et al.*, 2005). We found that the general *PIN3* (Fig. 4f, panels 1–4) and *PIN4* (Fig. S3d) expression pattern was maintained. This suggests that the IDS controlled by FPGS1 can be independent of auxin gradients. To confirm this, we grew the mutant seedlings in the presence of auxin and found no root growth recovery. General patterns of root growth inhibition and lateral root initiation induced by auxin were similar to those in WT (Fig. S5), further suggesting unaltered auxin responses in the mutant.

The indeterminacy-to-determinacy switch depends on folate status

In the *mko2* mutant the other two isoforms, FPGS2 and FPGS3, should maintain enzymatic activity to some extent, even though their transcript level is lower than in WT (Fig. 3c). As mentioned above, *mko2* seedlings re-established indeterminate primary root growth in the presence of 5-CHO-THF (Fig. S1f,g). RAM organization and the expression of the studied molecular markers and auxin transporters in *mko2* roots treated with 5-CHO-THF were also mainly re-established (Fig. 4, last two columns). Quantitative analysis showed that *pPLT1::CFP* fluorescence was re-established to the same level as in WT (Fig. 4c, insets in the last two columns). *DR5rev::GFP* and *pPIN3::PIN3::GFP* expression was more variable in *mko2* roots grown on media supplemented with 5-CHO-THF; however, no statistically significant difference in signal intensity was found compared with WT (Fig. 4d,f, insets in the last two columns). The *mko2* root growth recovery was similar to that observed in an allelic null mutant, *atdfb-1* (Srivastava *et al.*, 2011a), and therefore other FPGS isoforms may participate in re-establishment of folate metabolism in these allelic mutants. Considering that folates are essential for one-carbon metabolism and that methionine synthesis is C1-dependent (Ravanel *et al.*, 2011), we investigated whether *mko2* root growth can also be restored by methionine, similar to *atdfb-1* (Srivastava *et al.*, 2011a). We found that *mko2* determinate root growth became indeterminate, although the primary root growth rate was lower than in WT (Fig. S1h). This finding implies that the RAM function was at least in part compromised by deprivation of the C1 metabolism-dependent products. Therefore, we suggest that the FPGS1 function prevents RAM determinacy through both a specific requirement for FPGS1 in stem cell niche maintenance and a general role in maintenance of folate-dependent C1 metabolism. If the presence of folates is essential for indeterminate root growth, then inhibition of folate synthesis should cause root determinacy. To test this hypothesis, we grew WT seedlings in the medium supplemented with 25 nM methotrexate, a compound that strongly inhibits folate synthesis (Crosti, 1981; Appleman *et al.*, 1988; Prabhu *et al.*, 1998). We found that the primary root did not reach > 2 mm in length and all seedlings exhibited complete RAM exhaustion and determinate growth of the primary root (Fig. S6).

FPGS1 is also involved in lateral root primordium morphogenesis

FPGS1 activity was originally identified in plastids (Ravanel *et al.*, 2001). However, transient expression of *pFPGS1::FPGS1::GFP* in tobacco cultured cells showed GFP signal in both plastids and the cytosol (Srivastava *et al.*, 2011b). Using *pFPGS1::FPGS1::GFP*, we transformed *atdfb-1* and *mko2* mutants and detected GFP expression in the cytoplasm of the root tip cells. We also found that GFP expression was highest in the RAM of the primary root and LRs and in LR primordia (LRP) (Fig. S7). High *FPGS1* expression in the LRP prompted us to investigate whether FPGS1 has a role in LR development. We found an increase in the density of LR initiation events (for both LRs and LRP) in *mko2*. However, because the elongated cells were much shorter in both the *mko2* and *atdfb-3* mutants, the LR initiation index (Dubrovsky *et al.*, 2009) remained the same as in the respective WT (Fig. S8a–c). Therefore, LR initiation was not affected in *mko2*. However, the mutant seedlings showed delayed LR emergence. In WT and *mko2* seedlings at 6 dpg, emerged LRs represented 42% and 18% of all LR initiation events, respectively ($n = 237$ LR initiation events in 15 WT primary roots and 50 events in 16 *mko2* primary roots), indicating slower primordium development in the mutant. In *mko2* and *atdfb-3* mutants, a majority of the LR primordia were also abnormal (Fig. 6a). Defects in primordium morphogenesis in *mko2* were related to the disturbed balance between periclinal and anticlinal divisions: at the same developmental stage, in the external primordium cell layer a greater number of cells were found in *mko2* compared

with WT. Also, periclinal divisions in the external primordium layer were spread to a greater extent than in the WT, resulting in abnormal primordium shape (compare Fig. 6b,c). Neither *atdfc* nor *atdfd* mutants had these developmental abnormalities (Fig. S8f). Moreover, the LR initiation index in *atdfc* was similar to that in *mko2*, and a slight decrease was found in *atdfd* (Fig. S8c). These results demonstrated a nonredundant requirement for FPGS1 for LR primordium morphogenesis. In spite of the patterning abnormalities, emerged lateral roots had apparently indeterminate root growth. The time of emergence of individual LRs was recorded and their apices were analyzed under the microscope 20 d later. None of the LRs analyzed showed root determinacy ($n = 20$; Fig. S8d,e). Nevertheless, similarly to the primary root, LR growth was very slow in the *mko2* mutant and the whole root system still had not reached 5 mm in length at 15 dpg (data not shown).

Discussion

It was shown previously that folate polyglutamylation is important for root meristem maintenance (Srivastava *et al.*, 2011a). Here we extended this analysis and now provide compelling evidence that folate polyglutamate (vitamin B9) production represents a new pathway involved in IDS control. Interestingly, another vitamin (B6, pyridoxine) is also essential for root growth. A loss-of-function mutation in *PYRIDOXINE SYNTHASE 1* strongly inhibits *A. thaliana* root growth and diminishes meristem length but, in contrast to the *mko2* mutation, does not induce RAM consumption (Chen & Xiong, 2005). This and many other examples of reduced RAM length show that the developmental program for maintenance of meristem size is different from that for the maintenance of indeterminacy. When the former program is compromised, a smaller meristem is preserved, whereas when the latter program does not operate, the whole meristem becomes consumed. Therefore, the IDS represents a specific developmental pathway in the regulation of RAM behavior in general and we propose that it is a different level of regulation of root meristem development in addition to meristem maintenance.

A key question is whether the IDS in *mko2* was caused by a generally weakened metabolism resulting from disturbed C1 metabolism or whether it was specifically dependent on the role of FPGS1 in root development. We believe that both possibilities are valid. Comparison of *mko2* and *atdfb-1* versus the respective WT indicates that the *FPGS1* mutation in the Ler background led to a greater deficiency of polyglutamylated folates (21% and 69% of WT amounts were available in *mko2* and *atdfb-1* roots, respectively). This might explain the more drastic metabolic changes and stronger phenotype in *mko2* versus *atdfb-1*. A lower folate polyglutamylation level can impact one-carbon metabolism reactions as a result of decreased folate retention within compartments and because of the preference of many folate-utilizing enzymes for the polyglutamylated forms of folates. For example, methionine synthase does not have significant activity with monoglutamylated form of 5-CH3-THF (Ravanel *et al.*, 2004).

The *A. thaliana* primary root executes either indeterminate (under normal growth conditions) or determinate (under phosphate-deficiency conditions) developmental programs (Sánchez-Calderón *et al.*, 2005). At some developmental time, the transition from the indeterminate to the determinate program under low phosphate has a point of no return because no stem cells could maintain their function (Sánchez-Calderón *et al.*, 2005). Similar behavior was found in *mko2* when the mutant first grew in folate-free medium and then after different time intervals was transferred into folate-containing medium (data not shown). In this case, recovery was possible only when *mko2* seedlings were

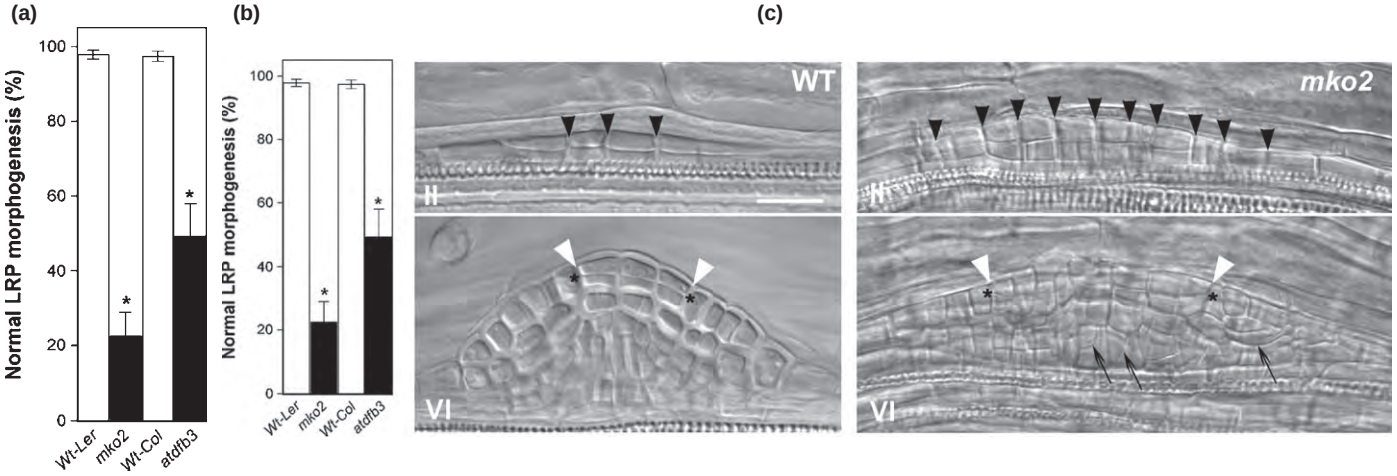

Fig. 6 FOLYLPOLYGLUTAMATE SYNTHETASE1 (FPGS1)/DIHYDROFOLATE SYNTHETASE-FPGS homolog B (AtDFB) is required for *Arabidopsis thaliana* lateral root primordium morphogenesis. (a) Percentage of lateral root primordia (LRP) with normal morphogenesis in *moots koom2* (*mko2*) and *atdfb-3* versus the respective wild type (WT). Mean ± SE for three samples, four seedlings each; number of primordia per sample was 10–18 (*mko2*) and 53–69 (WT). Statistically significant differences were determined using Student's *t*-test: *, $P < 0.05$. (b, c) Examples of abnormalities in primordium morphogenesis in *mko2* (c) as compared with WT Ler (b) at stages II and VI. Black arrowheads indicate anticlinal divisions that took place at stage I. White arrowheads show the portion of the primordium dome where in the external cell layer periclinal division took place. Asterisks show these periclinal divisions; arrows indicate abnormally oriented divisions. All the data are for seedlings at 6 d post-germination (dpg). Bar, 40 μm.

transferred before RAM exhaustion (Fig. S1f). These observations indicate that overall the IDS concept can be applied to both WT *A. thaliana* and the *mko2* mutant. The fact that WT plants could phenocopy *mko2* when treated with an inhibitor of folate synthesis (Fig. S6) suggests that endogenous folate levels are involved in the regulation of the transition from root indeterminacy to determinacy. Also, the correlation between a lower abundance of polyglutamylated folates and a stronger root phenotype in *mko2* in Ler versus *atdfb-3* in Col-0 (Fig. 2e) supports the possibility that folates emerge as endogenous regulators of the IDS in *A. thaliana*.

A puzzling question is how to explain the finding that exogenous treatment with 5-CHO-THF reversed determinate growth to indeterminate (Fig. S1f), whereas this same folate species accumulated endogenously in the mutant (Fig. 3b). A possible explanation could be related to compartmentalization of folate species essential for cell proliferation. 5,10-CH=THF is synthesized from 5-CHO-THF only in mitochondria and is a precursor for 10-CHO-THF, which donates C1 for synthesis of purine and formyl-methionyl-tRNA, required for DNA synthesis during cell cycle S-phase (Fig. 1; Ravanel *et al.*, 2011). The short-root phenotype in *mko2* suggests that the observed accumulation of 5-CHO-THF in the mutant tissues took place in compartments other than the mitochondria, where it could not be metabolized. However, when 5-CHO-THF is present in the growth medium at a high concentration, root growth is re-established. We hypothesize that this monoglutamylated folate species in the medium creates a stoichiometric shift, which partially recovers cellular folate metabolism with the aid of FPGS2 and three isoforms.

Stem cell niche behavior in the *mko2* mutant was remarkably similar to that in the *ccs52a2* mutant (Vanstraelen *et al.*, 2009): the QC cells became activated before RAM exhaustion, distal stem cells became differentiated, and PLT1 and WOX5 activities were present until RAM exhaustion. In both cases, abnormal QC function promotes distal stem cell differentiation, similar to laser-ablated QC cells (Van Den Berg *et al.*, 1997). However, it is worth noting that QC activation does not always lead to root determinacy. Ethylene also promotes QC cell division but its identity and function are maintained and no IDS is turned on (Ortega-Martínez *et al.*, 2007).

It has been previously shown that, in mutant seedlings showing root determinacy, cell division activity in the RAM and the cell proliferation domain can be present during a very narrow window of time, as in the *shr* (Lucas *et al.*, 2011) and *ccs52a2* (Vanstraelen *et al.*, 2009) mutants. Alternatively, it can be maintained for a more extended time before the determinacy program is turned on, as in the *scr* (Sabatini *et al.*, 2003) mutant. Interestingly, under natural conditions, as in the constitutively present determinacy program in Cactaceae, both scenarios are functional (Dubrovsky, 1997; Dubrovsky & Gomez-Lomeli, 2003; Shishkova *et al.*, 2013), suggesting that this developmental program does not depend on whether the RAM cells above the stem cell niche maintain cell division for a longer or shorter time. In *mko2*, meristematic cells were found in the root tip before RAM consumption, suggesting that during RAM exhaustion developmental changes in both the stem cell niche and the proliferation domain are taking place in a coordinated manner. Our data indicate that the maintenance of root indeterminacy and normal stem cell niche function is impossible without FPGS1 activity, while other regulatory modules involved in RAM maintenance are not affected.

The finding that the IDS was independent of auxin gradients in this study is in agreement with the absence of changes in auxin tissue content in *A. thaliana* seedlings treated with an inhibitor of THF biosynthesis (Stokes *et al.*, 2013). RAM exhaustion of the *A. thaliana* triple mutant in the GRAS transcription factors *HAIRY MERISTEM1*, *2*, and *3*, which also has root determinacy, is similarly independent of auxin gradients (Engstrom *et al.*, 2011). Nevertheless, we cannot exclude a link between folate metabolism and auxin signaling, specifically in the QC. High auxin concentrations and maximum response in the QC are involved in its function as a stem cell niche (Bennett & Scheres, 2010). Creation of this maximum depends on *WOX5*-regulated auxin synthesis in the QC cells, which in turn is IAA17-dependent (Tian *et al.*, 2013). The *mko2* mutant shows an expanded *WOX5* expression domain, similar to the *iaa17/axr3* mutant (Tian *et al.*, 2013), which could be related to IAA17 function and may suggest possible interactions between folate and auxin signaling pathways.

Interestingly, the IDS can be turned on in roots that show both a lower auxin content, as in *35S::PID* (Friml *et al.*, 2004), and a higher auxin content, as in *shr* (Lucas *et al.*, 2011), compared with WT. This also suggests that this developmental switch is not entirely auxin dependent. The auxin response and auxin transporter expression were maintained in the *mko2* and are in line with this idea. The fact that *FPGS1* is found among QC-enriched transcripts (Nawy *et al.*, 2005) and that it is highly expressed in cortex-endodermis initial cells and their daughters (Sozzani *et al.*, 2010) supports its pivotal role in stem cell niche function. Indeed, as shown here, the *mko2* QC loses its quiescence and this appears to be a critical step in the transition to RAM determinacy. Therefore, our data reinforce the concept that the QC is required for indeterminate root growth (Rodríguez-Rodríguez *et al.*, 2003; Sabatini *et al.*, 2003; Aida *et al.*, 2004). We show that this requirement is FPGS1 dependent.

FPGS1 is mainly involved in the root and not in the development of other plant organs. *FPGS1*, in contrast to *FPGS2* and *FPGS3*, is strongly expressed in the RAM and in the young differentiation zone of the root, with the highest expression level in the protoxylem-adjacent pericycle and LR primordium (Brady *et al.*, 2007; Winter *et al.*, 2007). Concordantly, FPGS1, but not FPGS2 or FPGS3 is co-expressed with other genes specifically in roots (Fig. S9, Table S1) and the phenotypes of loss-of-function mutants in other *FPGS* genes did not show abnormal root development (Mehrshahi *et al.*, 2010; Jiang *et al.*, 2013), similar to our root growth analysis (Fig. 2a). Moreover, we found abnormalities in LR primordium morphogenesis only in *fpgs1* mutants. In spite of the role of FPGS1 in LR development, no effect on LR initiation was found in the *mko2*, *atdfb-3*, and *atdfc* mutants. The decrease in the LR initiation index found in *atdfd* was only 23% (Fig. S8a–c). The fact that LR initiation was unaffected in

FPGS1 mutants suggests that the role of FPGS1 in root development is not related to a general inhibition of cell proliferation. Based on the number of LR initiation events, it has been reported that the *atdfc* mutant is impaired in LR initiation under nitrogen-limiting conditions (Jiang *et al.*, 2013). However, a comparison of the primary root length and the number of LR initiation events reported in this study shows that both parameters changed proportionally, indicating that LR initiation is not affected in *atdfc* either. Surprisingly, emerged LRs in *mko2* did not show determinacy (Fig. S8d,e) but their growth was inhibited to a comparable extent as that of the primary roots.

Based on the abnormal patterning of the primary root meristem, meristem exhaustion, defective LR primordium morphogenesis, and delayed LR emergence found in the *mko2* and *atdfb-3* mutants, FPGS1 emerges as an important player involved in root architecture development and plasticity. One component of root system architecture plasticity is determinacy of LRs, as in maize (*Zea mays*) plants (Varney & McCully, 1991). Our data suggest that FPGS1 can act as a potentially important player in the control of the IDS, and further studies are required to uncover its role in plant root system plasticity regulation in crops under natural growth conditions.

Acknowledgements

We thank B. García-Ponce, G. Cassab, and M. Rocha for discussion during the course of this work and S. Napsucialy-Mendivil, E. P. Rueda-Benitez, M. Ramírez-Yarza, A. Saralegui, J. A. Pimentel-Cabrera, J. Verleyen, L. Collado-Torres, A. Sharma, J. M. Hurtado-Ramírez and the staff of the UNAM DNA Deep Sequencing and DNA Synthesis Facilities for excellent technical help. We thank J. Bowman, B. Scheres, J. Friml and P. Benfey for seed donation, and the referees for valuable comments on the manuscript. This paper constitutes a partial fulfillment of the Graduate Program in Biomedical Sciences of the Universidad Nacional Autónoma de México (UNAM). B.J.R-H. acknowledges the scholarship and financial support provided by Consejo Nacional de Ciencia y Tecnología of Mexico (CONACyT). J-C.M. acknowledges a postdoctoral fellowship from Secretaría de Relaciones Exteriores of Mexican Government. This work was supported by the Dirección General de Asuntos del Personal Académico (UNAM-DGAPA) (postdoctoral fellowships to Y.U-C., V.L-R., and G.D.), UNAM-DGAPA-PAPIIT (grants IN204912 to S.S. and IN204312 to J.G.D.), CONACyT (grants 79736 to S.S. and 127957 to J.G.D), the Endowed Chair in Micronutrients (Tec. de Monterrey grant 0020CAT198 to R.I.D.G), and the BioEnergy Science Center of the US Department of Energy (grant to E.B.B.).

References

Aida M, Beis D, Heidstra R, Willemsen V, Blilou I, Galinha CR, Nussaume L, Noh Y-S, Amasino R, Scheres B. 2004. The *PLETHORA* genes mediate patterning of the *Arabidopsis* root stem cell niche. *Cell* **119**: 109–120.

Appleman JR, Prendergast N, Delcamp TJ, Freisheim JH, Blakley RL. 1988. Kinetics of the formation and isomerization of methotrexate complexes of recombinant human dihydrofolate reductase. *Journal of Biological Chemistry* **263**: 10304–10313.

Benfey PN, Linstead PJ, Roberts K, Schiefelbein JW, Hauser M-T, Aeschbacher RA. 1993. Root development in *Arabidopsis*: four mutants with dramatically altered root morphogenesis. *Development* **119**: 57–70.

Bennett T, Scheres B. 2010. Root development – two meristems for the price of one? In: Timmermans MCP, ed. *Current topics in developmental biology plant development*. San Diego, CA, USA: Academic Press, 67–102.

Blilou I, Xu J, Wildwater M, Willemsen V, Paponov I, Friml J, Heidstra R, Aida M, Palme K, Scheres B. 2005. The PIN auxin efflux facilitator network controls growth and patterning in *Arabidopsis* roots. *Nature* **433**: 39–44.

Brady SM, Orlando DA, Lee J-Y, Wang JY, Koch J, Dinneny JR, Mace D, Ohler U, Benfey PN. 2007. A high-resolution root spatiotemporal map reveals dominant expression patterns. *Science* **318**: 801–806.

Chen H, Xiong L. 2005. Pyridoxine is required for post-embryonic root development and tolerance to osmotic and oxidative stresses. *The Plant Journal* **44**: 396–408.

Cheng JC, Seeley KA, Sung ZR. 1995. *RML1* and *RML2*, *Arabidopsis* genes required for cell proliferation at the root tip. *Plant Physiology* **107**: 365–376.

Clough SJ, Bent AF. 1998. Floral dip: a simplified method for *Agrobacterium*-mediated transformation of *Arabidopsis thaliana*. *The Plant Journal* **16**: 735–743.

Crosti P. 1981. Effect of folate analogues on the activity of dihydrofolate reductases and on the growth of plant organisms. *Journal of Experimental Botany* **32**: 717–723.

Cruz-Ramírez A, Oropeza-Aburto A, Razo-Hernández F, Ramírez-Chavez E, Herrera-Estrella L. 2006. Phospholipase DZ2 plays an important role in extraplastidic galactolipid biosynthesis and phosphate recycling in *Arabidopsis* roots. *Proceedings of the National Academy of Sciences, USA* **103**: 6765–6770.

Curtis MD, Grossniklaus U. 2003. A gateway cloning vector set for high-throughput functional analysis of genes *in planta*. *Plant Physiology* **133**: 462–469.

Dubrovsky JG. 1997. Determinate primary-root growth in seedlings of Sonoran Desert Cactaceae; its organization, cellular basis, and ecological significance. *Planta* **203**: 85–92.

Dubrovsky JG, Gomez-Lomeli LF. 2003. Water deficit accelerates determinate developmental program of the primary root and does not affect lateral root initiation in a Sonoran Desert cactus (*Pachycereus pringlei*, Cactaceae). *American Journal of Botany* **90**: 823–831.

Dubrovsky JG, Soukup A, Napsucialy-Mendivil S, Jeknic Z, Ivanchenko MG. 2009. The lateral root initiation index: an integrative measure of primordium formation. *Annals of Botany* **103**: 807–817.

Engstrom EM, Andersen CM, Gumulak-Smith J, Hu J, Orlova E, Sozzani R, Bowman JL. 2011. *Arabidopsis* homologs of the *Petunia HAIRY MERISTEM* gene are required for maintenance of shoot and root indeterminacy. *Plant Physiology* **155**: 735–750.

Friml F, Vieten A, Sauer M, Weijers D, Schwarz H, Hamann T, Offringa R, Jürgens G. 2003. Efflux-dependent auxin gradients establish the apical-basal axis of *Arabidopsis*. *Nature* **426**: 147–153.

Friml J, Benková E, Blilou I, Wiśniewska J, Hamann T, Ljung K, Woody S, Sandberg G, Scheres B, Jürgens G, *et al.* 2002a. AtPIN4 mediates sink-driven auxin gradients and root patterning in *Arabidopsis*. *Cell* **108**: 661–673.

Friml J, Wiśniewska J, Benková E, Mendgen K, Palme K. 2002b. Lateral relocation of auxin efflux regulator PIN3 mediates tropism in *Arabidopsis*. *Nature* **415**: 806–809.

Friml J, Yang X, Michniewicz M, Weijers D, Quint A, Tietz O, Benjamins R, Ouwerkerk PBF, Ljung K, Sandberg G, *et al.* 2004. A PINOID-dependent binary switch in apical-basal PIN polar targeting directs auxin efflux. *Science* **306**: 862–865.

Galinha C, Hofhuis H, Luijten M, Willemsen V, Blilou I, Heidstra R, Scheres B. 2007. PLETHORA proteins as dose-dependent master regulators of *Arabidopsis* root development. *Nature* **449**: 1053–1057.

Hanson AD, Gregory JF III. 2011. Folate biosynthesis, turnover, and transport in plants. *Annual Review of Plant Biology* **62**: 105–125.

Heidstra R, Welch D, Scheres B. 2004. Mosaic analyses using marked activation and deletion clones dissect *Arabidopsis* SCARECROW action in asymmetric cell division. *Genes & Development* **18**: 1964–1969.

Hernández-Barrera A, Ugartechea-Chirino Y, Shishkova S, Napsucialy-Mendivil S, Soukup A, Reyes-Hernández BJ, Lira-Ruan V, Dong G, Dubrovsky JG. 2011. Apical meristem exhaustion during determinate primary root growth in the *moots koom 1* mutant of *Arabidopsis thaliana*. *Planta* **234**: 1163–1177.

Ifergan I, Assaraf YG. 2008. Molecular mechanisms of adaptation to folate deficiency. In: Litwack G, ed. *Folic acid and folates*. London, UK: Academic Press, 99–143.

Ishikawa T, Machida C, Yoshioka Y, Kitano H, Machida Y. 2003. The *GLOBULAR ARREST1* gene, which is involved in the biosynthesis of folates, is essential for embryogenesis in *Arabidopsis thaliana*. *The Plant Journal* **33**: 235–244.

Ivanov VB, Dubrovsky JG. 2013. Longitudinal zonation pattern in plant roots: conflicts and solutions. *Trends in Plant Science* **18**: 237–243.

Jiang L, Liu Y, Sun H, Han Y, Li J, Li C, Guo W, Meng H, Li S, Fan Y, *et al.* 2013. The mitochondrial folylpolyglutamate synthetase gene is required for nitrogen utilization during early seedling development in *Arabidopsis*. *Plant Physiology* **161**: 971–989.

Kooke R, Keurentjes JJB. 2012. Multi-dimensional regulation of metabolic networks shaping plant development and performance. *Journal of Experimental Botany* **63**: 3353–3365.

Lucas M, Swarup R, Paponov IA, Swarup K, Casimiro I, Lake D, Peret B, Zappala S, Mairhofer S, Whitworth M, *et al.* 2011. Short-Root regulates primary, lateral, and adventitious root development in *Arabidopsis*. *Plant Physiology* **155**: 384–398.

Mehrshahi P, González-Jorge S, Akhtar TA, Ward JL, Santoyo-Castelazo A, Marcus SE, Lara-Núñez A, Ravanel S, Hawkins ND, Beale MH. 2010. Functional analysis of folate polyglutamylation and its essential role in plant metabolism and development. *The Plant Journal* **64**: 267–279.

Mo X, Zhu Q, Li X, Li J, Zeng Q, Rong H, Zhang H, Wu P. 2006. The *hpa1* mutant of *Arabidopsis* reveals a crucial role of histidine homeostasis in root meristem maintenance. *Plant Physiology* **141**: 1425–1435.

Nakajima K, Sean G, Nawy T, Benfey PN. 2001. Intercellular movement of the putative transcription factor SHR in root patterning. *Nature* **413**: 307–311.

Nawy T, Lee JY, Colinas J, Wang JY, Thongrod SC, Malamy JE, Birnbaum K, Benfey PN. 2005. Transcriptional profile of the *Arabidopsis* root quiescent center. *The Plant Cell* **17**: 1908–1925.

Ortega-Martínez O, Pernas M, Carol RJ, Dolan L. 2007. Ethylene modulates stem cell division in the *Arabidopsis thaliana* root. *Science* **317**: 507–510.

Pérez-Pérez JM, Serralbo O, Vanstraelen M, González C, Criqui MC, Genschik P, Kondorosi E, Scheres B. 2008. Specialization of CDC27 function in the *Arabidopsis thaliana* anaphase-promoting complex (APC/C). *The Plant Journal* **53**: 78–89.

Perilli S, Di Mambro R, Sabatini S. 2012. Growth and development of the root apical meristem. *Current Opinion in Plant Biology* **15**: 17–23.

Petersson SV, Johansson AI, Kowalczyk M, Makoveychuk A, Wang JY, Moritz T, Grebe M, Benfey PN, Sandberg G, Ljung K. 2009. An auxin gradient and maximum in the *Arabidopsis* root apex shown by high-resolution cell-specific analysis of IAA distribution and synthesis. *The Plant Cell* **21**: 1659–1668.

Prabhu V, Brock Chatson K, Lui H, Abrams GD, King J. 1998. Effects of sulfanilamide and methotrexate on 13C fluxes through the glycine decarboxylase/serine hydroxymethyltransferase enzyme system in *Arabidopsis*. *Plant Physiology* **116**: 137–144.

Ramakers C, Ruijter JM, Deprez RHL, Moorman AF. 2003. Assumption-free analysis of quantitative real-time polymerase chain reaction (PCR) data. *Neuroscience letters* **339**: 62–66.

Ravanel S, Block MA, Rippert P, Jabrin S, Curien G, Rébeillé F, Douce R. 2004. Methionine metabolism in plants: chloroplasts are autonomous for *de novo* methionine synthesis and can import S-adenosylmethionine from the cytosol. *Journal of Biological Chemistry* **279**: 22548–22557.

Ravanel S, Cherest H, Jabrin S, Grunwald D, Surdin-Kerjan Y, Douce R, Rébeillé F. 2001. Tetrahydrofolate biosynthesis in plants: molecular and functional characterization of dihydrofolate synthetase and three isoforms of folylpolyglutamate synthetase in *Arabidopsis thaliana*. *Proceedings of the National Academy of Sciences, USA* **98**: 15360–15365.

Ravanel S, Douce R, Rébeillé F. 2011. Metabolism of folates in plants. In: Rebeille F, Douce R, eds. *Advances in botanical research*. London, UK: Academic Press, 67–106.

Rodríguez-Rodríguez JF, Shishkova S, Napsucialy-Mendivil S, Dubrovsky JG. 2003. Apical meristem organization and lack of establishment of the quiescent center in Cactaceae roots with determinate growth. *Planta* **217**: 849–857.

Sabatini S, Beis D, Wolkenfelt H, Murfett J, Guilfoyle T, Malamy J, Benfey P, Leyser O, Bechtold N, Weisbeek P, *et al.* 1999. An auxin-dependent distal organizer of pattern and polarity in the *Arabidopsis* root. *Cell* **99**: 463–472.

Sabatini S, Heidstra R, Wildwater M, Scheres B. 2003. SCARECROW is involved in positioning the stem cell niche in the *Arabidopsis* root meristem. *Genes and Development* **17**: 354–358.

Sánchez-Calderón L, López-Bucio J, Chacón-López A, Cruz-Ramirez A, Nieto-Jacobo F, Dubrovsky JG, Herrera-Estrella L. 2005. Phosphate starvation induces a determinate developmental program in the roots of *Arabidopsis thaliana*. *Plant and Cell Physiology* **46**: 174–184.

Sanghani SP, Sanghani PC, Moran RG. 1999. Identification of three key active site residues in the C-terminal domain of human recombinant folylpoly-gamma-glutamate synthetase by site-directed mutagenesis. *Journal of Biological Chemistry* **274**: 27018–27027.

Sarkar AK, Luijten M, Miyashima S, Lenhard M, Hashimoto T, Nakajima K, Scheres B, Heidstra R, Laux T. 2007. Conserved factors regulate signalling in *Arabidopsis thaliana* shoot and root stem cell organizers. *Nature* **446**: 811–814.

Schneeberger K, Ossowski S, Lanz C, Juul T, Petersen AH, Nielsen KL, Jørgensen JE, Weigel D, Andersen SU. 2009. SHOREmap: simultaneous mapping and mutation identification by deep sequencing. *Nature Methods* **6**: 550–551.

Shane M, Lambers H. 2005. Cluster roots: a curiosity in context. *Plant and Soil* **274**: 101–125.

Shishkova S, Las Peñas ML, Napsucialy-Mendivil S, Matvienko M, Kozik A, Montiel J, Patiño A, Dubrovsky JG. 2013. Determinate primary root growth as an adaptation to aridity in Cactaceae: towards an understanding of the evolution and genetic control of the trait. *Annals of Botany* **112**: 239–252.

Shishkova S, Rost TL, Dubrovsky JG. 2008. Determinate root growth and meristem maintenance in angiosperms. *Annals of Botany* **101**: 319–340.

Sozzani R, Cui H, Moreno-Risueno M, Busch W, Van Norman J, Vernoux T, Brady S, Dewitte W, Murray J, Benfey P. 2010. Spatiotemporal regulation of cell-cycle genes by SHORTROOT links patterning and growth. *Nature* **466**: 128–132.

Srivastava AC, Ramos-Parra PA, Bedair M, Robledo-Hernández AL, Tang Y, Sumner LW, de la Garza RID, Blancaflor EB. 2011a. The folylpolyglutamate synthetase plastidial isoform is required for postembryonic root development in *Arabidopsis*. *Plant Physiology* **155**: 1237–1251.

Srivastava AC, Tang Y, de la Garza RID, Blancaflor EB. 2011b. The plastidial folylpolyglutamate synthetase and root apical meristem maintenance. *Plant Signaling & Behavior* **6**: 751–754.

Stepanova AN, Robertson-Hoyt J, Yun J, Benavente LM, Xie DY, Dolezal K, Schlereth A, Jürgens G, Alonso JM. 2008. TAA1-mediated auxin biosynthesis is essential for hormone crosstalk and plant development. *Cell* **133**: 177–191.

Stokes ME, Chattopadhyay A, Wilkins O, Nambara E, Campbell MM. 2013. Interplay between sucrose and folate modulates auxin signaling in *Arabidopsis*. *Plant Physiology* **162**: 1552–1565.

Svistoonoff S, Creff A, Reymond M, Sigoillot-Claude C, Ricaud L, Blanchet A, Nussaume L, Desnos T. 2007. Root tip contact with low-phosphate media reprograms plant root architecture. *Nature genetics* **39**: 792–796.

Swarup R, Friml J, Marchant A, Ljung K, Sandberg G, Palme K, Bennett M. 2001. Localization of the auxin permease AUX1 suggests two functionally distinct hormone transport pathways operate in the *Arabidopsis* root apex. *Genes & Development* **15**: 2648–2653.

Tian H, Wabnik K, Niu T, Li H, Yu Q, Pollmann S, Vanneste S, Govaerts W, Rolčík J, Geisler M. 2013. WOX5-IAA17 feedback circuit mediated cellular auxin response is crucial for the patterning of root stem cell niches in *Arabidopsis*. *Molecular Plant* **7**: 277–289.

Van Den Berg C, Willemsen V, Hendriks G, Weisbeek P, Scheres B. 1997. Short-range control of cell differentiation in the *Arabidopsis* root meristem. *Nature* **390**: 287–289.

Vanstraelen M, Baloban M, Da Ines O, Cultrone A, Lammens T, Boudolf V, Brown SC, De Veylder L, Mergaert P, Kondorosi E. 2009. APC/CCCS52A complexes control meristem maintenance in the *Arabidopsis* root. *Proceedings of the National Academy of Sciences, USA* **106**: 11806–11811.

Varney G, McCully M. 1991. The branch roots of *Zea*. II. Developmental loss of the apical meristem in field-grown roots. *New Phytologist* **118**: 535–546.

Vernoux T, Wilson RC, Seeley KA, Reichheld JP, Muroy S, Brown S, Maughan SC, Cobbett CS, Montagu MV, Inz D, *et al.* 2000. The *ROOT MERISTEMLESS1/CADMIUM SENSITIVE2* gene defines a glutathione-dependent pathway involved in initiation and maintenance of cell division during postembryonic root development. *The Plant Cell* **12**: 97–109.

Watt M, Evans JR. 1999. Linking development and determinacy with organic acid efflux from proteoid roots of white lupin grown with low phosphorus and ambient or elevated atmospheric CO_2 concentration. *Plant Physiology* **120**: 705–716.

Willemsen V, Wolkenfelt H, de Vrieze G, Weisbeek P, Scheres B. 1998. The *HOBBIT* gene is required for formation of the root meristem in the *Arabidopsis* embryo. *Development* **125**: 521–531.

Winter D, Vinegar B, Nahal H, Ammar R, Wilson GV, Provart NJ. 2007. An "Electronic Fluorescent Pictograph" browser for exploring and analyzing large-scale biological data sets. *PLoS ONE* **2**: e718.

Xiong Y, McCormack M, Li L, Hall Q, Xiang C, Sheen J. 2013. Glucose-TOR signalling reprograms the transcriptome and activates meristems. *Nature* **496**: 181–186.

Zimmermann P, Hirsch-Hoffmann M, Hennig L, Gruissem W. 2004. GENEVESTIGATOR. Arabidopsis microarray database and analysis toolbox. *Plant Physiology* **136**: 2621–2632.

Zobel RW. 2013. Modeling *Lolium perenne* L. roots in the presence of empirical black holes. In: Timlin D, Ahuja LR, eds. *Advances in agricultural systems modeling 4. Enhancing understanding and quantification of soil–root growth interactions.* Madison, WI, USA: ASA, CSSA and SSS Press, 155–171.

Supporting Information

Additional supporting information may be found in the online version of this article.

Fig. S1 Phenotype of the *mko2* mutant plants and complementation tests.

Fig. S2 Multiple alignment of an FPGS conserved region close to the catalytic domain.

Fig. S3 Disorganization of the *mko2* primary root apical meristem.

Fig. S4 Disorganization in the primary root apical meristem of the *atdfb-1* mutant is similar to that of the *mko2* mutant.

Fig. S5 Analysis of *mko2* root development in the presence of 1-naphthalene acetic acid (NAA).

Fig. S6 Methotrexate-treated wild-type primary roots phenocopy *mko2* determinate root growth.

Fig. S7 *FPGS1/AtDFB* expression pattern in the root.

Fig. S8 Lateral root development in loss-of-function mutants in *FPGS1*, *2*, and *3* genes**.**

Fig. S9 Bioinformatics analysis of genes co-expressed with *FPGS1*, *2*, and *3* in the root.

Table S1 Genes coexpressed with *FPGS1*, *2* and *3* in roots in accordance with GENEVESTIGATOR

Please note: Wiley Blackwell are not responsible for the content or functionality of any supporting information supplied by the authors. Any queries (other than missing material) should be directed to the *New Phytologist* Central Office.